Ultrasonic assisted creep feed grinding of gamma titanium aluminide using conventional and superabrasive wheels

7 authors, including:

Debajyoti Bhaduri
Cardiff University
30 PUBLICATIONS   **223** CITATIONS

SEE PROFILE

Stefan Bohr
Saint-Gobain
14 PUBLICATIONS   **435** CITATIONS

SEE PROFILE

Some of the authors of this publication are also working on these related projects:

Project   Ecolaserfact View project

Project   Hyproline View project

Ultrasonic assisted creep feed grinding of gamma titanium aluminide using conventional and superabrasive wheels

Bhaduri, Debajyoti; Soo, Sein; Aspinwall, David; Novovic, Donka; Bohr, Stefan; Harden, Peter; Webster, John A.

[Link to publication on Research at Birmingham portal](#)

Ultrasonic assisted creep feed grinding of gamma titanium aluminide using conventional and superabrasive wheels

Debajyoti Bhaduri [a], Sein Leung Soo (2)[a], David K. Aspinwall (1)[a,*], Donka Novovic [b], Stefan Bohr [c], Peter Harden [a,1], John A. Webster (1)[d]

[a] Machining Research Group, Department of Mechanical Engineering, School of Engineering, University of Birmingham, Edgbaston, Birmingham, B15 2TT, UK
[b] Manufacturing Technology, Global Manufacturing Centre, Rolls-Royce plc, Derby, DE24 8ER, UK
[c] Saint-Gobain Diamantwerkzeuge GmbH, Schützenwall 13-17, D-22844 Norderstedt, Germany
[d] Cool-Grind Technologies, Ashford, Connecticut, 06278, USA

[1] Previously at Element Six Ltd. at the time the research was performed

The paper details experimental work on ultrasonic assisted creep feed grinding (UACFG) of γ-TiAl intermetallic alloy: Ti-45Al-2Mn-2Nb+0.8vol.%TiB$_2$XD (wt%), using conventional SiC and electroplated diamond wheels. The majority of forces recorded were lower when using vibration assistance compared to conventional CFG by up to ~35%, while grinding-ratios for the superabrasive wheel were substantially higher by a factor of 2-7. A reduction in workpiece surface roughness by up to ~10% together with fewer defects and marginally increased subsurface microhardness by a maximum of ~8%, was obtained when employing ultrasonic assistance. With uprated process parameters however, the effects of UACFG were less apparent.

1. Introduction

Despite the potential for gamma titanium aluminide (γ-TiAl) intermetallic alloys to replace heavier nickel based superalloy components such as turbine and compressor blades in gas turbine aeroengines, few civil or military applications currently exist. Several factors are responsible, not least the lack of a comprehensive material supply base and the requirement for stringent safety standards, but also alloy sensitivity to secondary production/manufacturing methods and associated post processing costs [1]. Key conventional machining operations for blades include high speed milling and grinding, the latter proving less of a problem in terms of machinability and the generation of acceptable workpiece surface integrity, due in part to the low room temperature ductility (~2%) of many γ-TiAl alloys [2]. While several researchers have shown the feasibility of creep feed grinding (CFG) γ-TiAl, published results highlight the need for reduced operating levels in order to achieve the necessary workpiece integrity, thus compromising productivity [3, 4].

The use of ultrasonic (US) vibration (> 20 kHz frequency) to aid machining appeared in the late 1920's with the development of US assisted grinding following in the 1950's. A comprehensive review of 'hybrid' machining processes including those associated with vibration/US assistance is detailed by Lauwers et al. [5]. The majority of published work on ultrasonic assisted grinding (UAG) has shown significant reductions in grinding forces and benefits in relation to cutting temperature, together with an improvement in workpiece surface integrity [6]. To date, UAG has largely been applied on some ceramics [7], glass and ferrous based materials [8], with only limited literature involving advanced aerospace alloys. In addition, commercial turn-key equipment is scarce. Work on UAG has mainly been associated with surface grinding configurations with depths of cut typically limited to ≤ 0.3 mm. Relatively few papers have reported hybrid ultrasonic assisted

creep feed grinding (UACFG) with depths of cut ≥ 1 mm [9, 10]. The present research aimed to investigate the effects of US vibration with regard to grinding productivity, wheel wear, cutting forces and workpiece integrity when CFG a γ-TiAl alloy using conventional and superabrasive wheels.

2. Experimental details

Blocks of Ti-45Al-2Mn-2Nb+0.8 vol.%TiB$_2$XD (wt%) γ-TiAl alloy (100 × 55 × 7 mm) were used as the workpiece material. This was produced by casting followed by hot isostatic pressing (HIPing) at a temperature of 1480°C and pressure of 148 MPa for 4 hours and subsequently heat treated at a temperature of 1050-1080°C, for 24 hours, giving a bulk hardness of ~365 HV$_{30}$. The material had a nearly fully lamellar structure with parallel plates of γ-TiAl and α_2-Ti$_3$Al, and a colony size of ~100-130 μm, see Fig. 1(a). The workpiece was clamped onto a specially designed aluminium table sonotrode/horn connected to an ultrasonic transducer ~20 kHz starting frequency linked to a multi-frequency, modulated ultrasonic generator rated at 1 kW. The primary direction of ultrasonic vibration was parallel to that of grinding feed (Y-axis). Under zero-load condition, a maximum amplitude of 8 μm was measured using a Laser Doppler Vibrometer.

All grinding trials were carried out on a Bridgeport FGC1000 flexible grinding centre, with a maximum spindle speed of 6000 rpm and power rating of 25 kW. Two high pressure pumping systems were utilised for delivery of grinding fluid via laminar flow nozzles with rectangular cross-sectioned outlets for cooling and cleaning the wheel during grinding [11]. The cooling nozzle orifice (2 x 20 mm) was directed towards the grinding zone at an angle and distance of 20° and 170 mm respectively, while the cleaning nozzle was aimed tangentially at the periphery on the opposite side of the wheel. Fluid pressure for cooling was 28 bar in order to match or exceed wheel velocity. In contrast, fluid pressure for cleaning was kept constant at 70 bar in all trials. The

grinding fluid employed was a water based synthetic oil product with a concentration of ~8 vol%. Plain profile vitrified bonded SiC and unconditioned electroplated (EP) diamond superabrasive wheels were utilised. Both wheels had similar average grit size of ~250 μm with an outer diameter and width of 220 mm and 20 mm respectively. An on-machine configuration of the SiC wheel-workpiece-sonotrode arrangement is shown in Fig. 1(b).
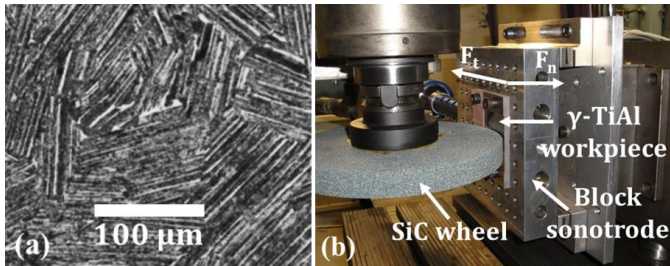
Fig. 1. (a) Microstructure of γ-TiAl; (b) wheel-workpiece-sonotrode assembly and force directions.

Phase 1 grinding trials involved the SiC wheel and a full factorial experimental array with 8 tests allowing variations in wheel velocity, v_s (15 and 30 m/s), table feed, v_w (150 and 600 mm/min) and ultrasonic vibration assistance (US ON and US OFF). Depth of cut per pass, a_e was fixed at 1 mm with all trials performed in a down grinding mode without spark-out. Wheel dressing was carried out prior to each trial using a diamond roller dresser with a 2 μm/rev infeed rate, 50 μm dressing depth and 0.8 dresser-to-wheel speed ratio. Phase 2 testing involved use of a superabrasive wheel to assess the influence of ultrasonic actuation. An initial series of 4 tests alternating between conventional CFG and UACFG were undertaken at fixed parameters v_s, v_w and a_e of 30 m/s, 150 mm/min and 1 mm respectively. Two additional tests (US ON and US OFF) were subsequently conducted at increased v_s and v_w of 40 m/s and 600 mm/min respectively. Each test in Phase 1 and 2 involved a single pass of the workpiece (55 mm cut length).

Grinding forces F_t and F_n, see Fig. 1(b), were measured using a Kistler 9257A dynamometer. Grinding-ratio was determined by measuring the wheel diameters before and after each test using a coordinate measuring machine. The wheels were assessed at 30 different points around the periphery, each at 5 different levels of the wheel width. Roughness of the ground workpieces (average of 3 measurements at start, middle and end of slot) was recorded using a stylus based profilometer, with 0.8 mm cut-off and 4 mm evaluation length. Wheel surface topography was assessed with a JEOL 6060 SEM by producing positive replicas using a synthetic rubber and resin replicating compound (Microset).

Knoop microhardness depth profile measurements of the γ-TiAl workpieces were taken using a 25 g load and indent time of 15 s. Three measurements were recorded, both in the transverse feed (TF) and longitudinal feed (LF) directions, each set at 10 μm depth intervals. In order to reveal workpiece microstructures, γ-TiAl samples were immersion etched in a solution of 2% hydrofluoric and 10% nitric acid with balance water for 5 s and were analysed using a Leica DMLM optical microscope.

3. Results and discussion

Figure 2(a) shows that the maximum F_n varied from ~1450 to 2300 N for the vitrified SiC wheel, with values increasing with cutting speed, the data being comparable to that reported by Hood et al. [4] when creep feed grinding γ-TiAl at similar process parameters. Analysis of variance (ANOVA) highlighted v_s as a significant factor at the 5% level with a percentage contribution ratio (PCR) of 83%, which was in line with previous work [4, 12].

This was attributed to an increase in the sliding length per unit volume of material removed when grinding at higher v_s, which resulted in greater attritious wear and dulling of the abrasive grits leading to higher rubbing and ploughing. Operation under UACFG generally led to lower F_n, while variation in v_w from 150 to 600 mm/min had minimal influence (based on tabulated data and corresponding main effects plots not shown here). Conversely, mean F_t, decreased with an increase in v_s and use of ultrasonic vibration (statistically significant with PCR of 64.5%). The application of US actuation generally led to reductions in both F_n and F_t by up to 19% and 35% respectively, possibly due to self-sharpening of the abrasive grains. Similar results were also presented by Nik et al. [13] when surface grinding Ti-6Al-4V alloy with a vitrified alumina wheel.
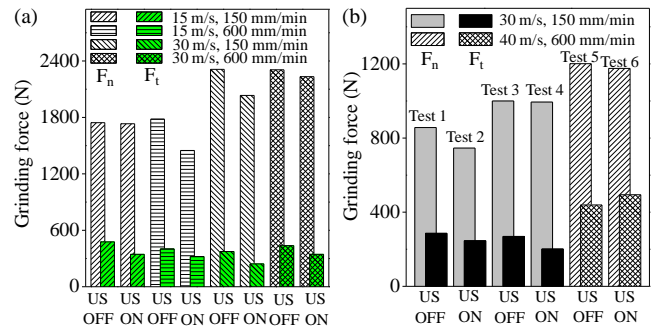
Fig. 2. (a) Grinding forces (F_n, F_t) when grinding with SiC wheel; (b) Grinding forces when using the EP diamond wheel.

In CFG tests with the superabrasive wheel (Tests 1, 3 and 5), F_n increased from 857 to 1200 N, the rise of ~150 N occurring between Test 1 and Test 3 due to cumulative wear of the wheel, see Fig. 2(b). A further increase of ~200 N between Test 3 and 5 was attributed to the elevated operating parameters (40 m/s and 600 mm/min). Despite the 13% reduction in F_n between Tests 1 (US OFF) and 2 (US ON), the application of ultrasonic vibration appeared to have minimal effect in succeeding tests, possibly due to the different dynamic/mass characteristics of the EP diamond wheel (steel hub) compared to the solid SiC wheel structure. Similarly, it is likely that the variation observed in F_t was due both to wheel wear and operating parameter variation rather than application of US assistance. With regard to the latter, Zhang and Zhang [14] reported that there is a critical value of feed rate above which the effect of ultrasonic vibration is diminished.

Figure 3(a) shows that the G-ratio of the SiC wheel varied from 3.2 to 8. This was similar to results by Hood et al. [4] where G-ratios between 2 to 15 were obtained when CFG a slightly different γ-TiAl alloy of Ti–45Al–8Nb–0.2C wt% using conventional SiC abrasives. Except for trials using the highest operating parameters (30 m/s and 600 mm/min), wheel wear increased (G-ratio reduced) with the rise of both v_s and v_w, while use of UACFG reduced wheel wear. This was most likely due to an increase in attritious wear at a higher cutting speed coupled with larger undeformed chip thickness, h_m at a greater table feed leading to more frictional forces. The increase in G-ratio (~30 to 75%) when using US assistance was possibly due in part to a reduction in thermal load. When evaluating the post-grinding wheel surfaces, large voids/loss of grits were typically seen following CFG as shown in Fig. 4(a). Conversely, the wheel surface appeared to be relatively uniform when operating under UACFG with only minor loss of grains, see Fig. 4(b). With uprated operating values, it is likely that the influence of US vibration was negated due to the additional loading on the system.

The comparatively high initial radial wear (~7 μm) of the EP diamond wheel after Test 1 under CFG as shown in Fig. 3(b), was due to conditioning of the protruding grits, which is typical with

new wheels. Wheel wear decreased to only ~2 μm in Test 3 as the majority of the protruding grits had undergone micro-fracture above the bond level. Signs of wear flats are shown in Fig. 4(c), however wheel surfaces generally exhibited no visible evidence of chip loading and/or adhered material at the tip of the grits or at inter-grit spaces. The marginal increase in wheel wear following Test 5 was the result of increasing v_s to 40 m/s, which would be expected to generate higher temperatures. Radial wheel wear remained almost negligible (~1 μm) in all UACFG trials, aided by the somewhat lower forces under hybrid conditions.
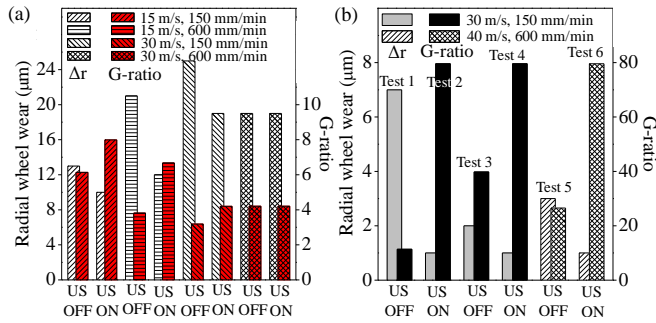

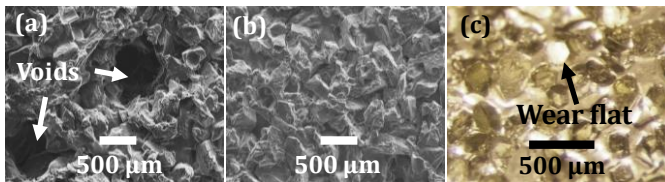**Fig. 3.** Radial wheel wear and G-ratio of (a) SiC; (b) diamond wheels.

Fig. 4. SEM micrographs of SiC wheel replicas after (a) CFG and (b) UACFG – both at v_s = 30 m/s, v_w = 150 mm/min; and (c) optical image of diamond wheel surface indicating a wear flat.

In contrast to the G-ratios obtained with the SiC wheel (~3 to 8), the diamond wheel produced higher values, in the range ~11-80. With CFG, these varied between ~11 and 40, with the lowest value in Test 1 reflecting the high initial radial/conditioning wear. Conversely, the G-ratios remained almost constant at ~80 under hybrid operation, regardless of operating parameters.

Minor burn and serration marks were observed when grinding with the SiC wheel at v_s=30 m/s, v_w=150 mm/min and US OFF, most likely due to generation of elevated temperatures when operating at the highest wheel speed, see Fig. 5(a). Work reported by Hood et al. [4] when CFG Ti–45Al–8Nb–0.2C wt% at a comparable v_s and v_w but higher depth of cut (2.5 mm), details moderate workpiece burn and extensive crack formation, albeit after 24,000 mm³ removed and a relatively low coolant pressure of 7 bar. The use of ~28 bar in the present study would be expected to lead to greater penetration of fluid into the grinding zone, thereby reducing temperatures. No workpiece burn was visible in any of the current trials with US actuation, see Fig. 5(b).
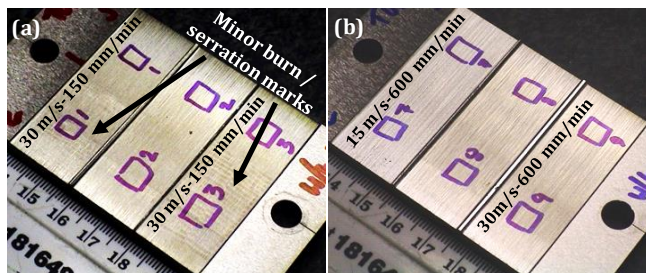

Fig. 5. Images of ground workpieces using SiC involving; (a) CFG – 30 m/s, 150 mm/min, (b) UACFG – 15 and 30 m/s, 600 mm/min.

High resolution SEM images of the ground surfaces revealed surface fracture and redeposited material on workpieces produced under conventional CFG conditions, see Figs. 6(a) and 6(b). No such damage however was apparent on any of the workpieces subject to UACFG, although greater side flow/ploughing of material and overlapping grit marks were evident on surfaces ground with both types of wheel as detailed in Figs. 6(c) and 6(d). This could have been due to a change in material removal mechanism from a fracture based regime to a ductile mode, as explained by Gao et al. [15] when UAG nano-zirconia ceramics. When ultrasonic assisted turning Ti-45Al-2Mn-2Nb+0.8vol.%TiB$_2$XD, Sharman et al. [16] reported that segmented continuous helical chips up to 25 mm long were produced in comparison to the more standard needle/discontinuous swarf associated with γ-TiAl alloys. It was also suggested that reduced cutting force would result in lower tensile stress in the shear zone, thereby reducing crack propagation and growth as normally seen with brittle materials. Additionally, it is feasible that the greater incidence of overlapping grit marks was in part caused by lateral movement of the abrasives [8] under possible multi-modal vibration.
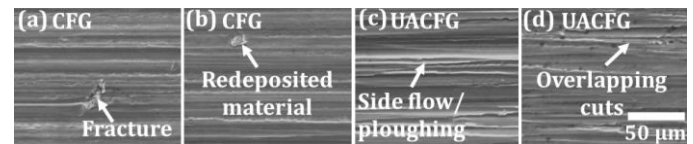

Fig. 6. SEM micrographs of γ-TiAl surfaces ground using SiC under (a) and (b) CFG; (c) and (d) UAG conditions.

Average surface roughness (R$_a$) for slots ground with the SiC wheel are shown in Fig. 7(a), which ranged from 1.56 to 2 μm R$_a$, in line with previous work [4]. Variation in v_w from 150 to 600 mm/min typically caused a rise in R$_a$ due to an increase in h$_m$, but decreased as v_s changed from 15 to 30 m/s (statistically significant with a PCR of 76.6%), due to a reduction of the number of grits in contact with the workpiece surface. Typically R$_a$ reduced by up to ~10% when utilising ultrasonic vibration in comparison to that obtained with conventional CFG, which was likely the result of increased active grains as well as overlapping grit trajectories in the former. This was in contrast to the increase in roughness observed when UACFG Inconel 718 [9, 10]. This could be attributed to the lamellar microstructure of γ-TiAl as opposed to the polycrystalline nature of Inconel 718, together with the higher fatigue crack growth rate, lower fracture toughness and impact resistance of γ-TiAl in comparison to Ni-alloys, resulting in easier material removal from the intermetallic workpieces under the impact-loading action of vibration.
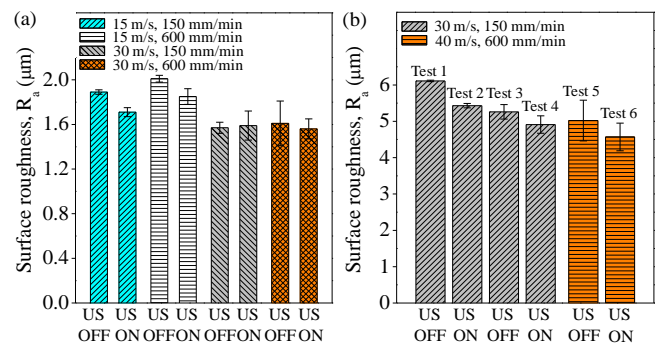

Fig. 7. Roughness (R$_a$) of γ-TiAl ground with (a) SiC; (b) diamond wheels.

With the EP diamond wheel, significantly higher workpiece roughness values were obtained compared to those with the SiC wheel due to the initially unconditioned nature of the former.

Average roughness gradually decreased from Test 1 to Test 4, see Fig. 7(b), due to use and engagement of a greater number of grits in cutting. However, R_a marginally increased in Test 5 due to an increase in v_w, but subsequently decreased following Test 6, although whether this was a result of further wheel wear/conditioning or micro-splintering of grits caused by US vibration as seen in Phase 1 trials with the SiC wheel, is unclear.

Figure 8 shows microhardness depth profile data for surfaces in the TF direction ground using the SiC wheel and LF direction ground using the EP diamond wheel. In the former case, maximum near surface (at ~10 μm) hardness ranged up to ~585 $HK_{0.025}$, falling to near the bulk hardness after depth of ~200 to 300 μm. Similar results have been reported by other authors when CFG γ-TiAl using SiC wheels [3, 12]. With ultrasonic assistance, subsurface microhardness typically increased by only ~6-8%, compared to conventional CFG. While the SEM micrographs of surfaces produced with UACFG showed greater ploughing/side flow and smearing of material, see Figs. 6(c) and 6(d), conclusive evidence of significantly increased plastic deformation/strain hardening due to ultrasonic assistance was not apparent in cross-sectional microstructures.
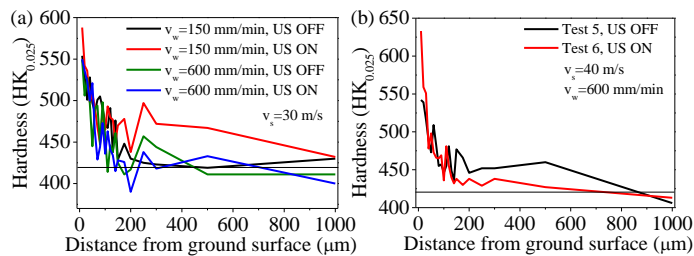
Fig. 8. Microhardness depth profiles of γ-TiAl in; (a) TF plane, ground using SiC wheel; (b) LF plane, ground using diamond wheel.

Figure 9(a) details a representative cross-sectional microstructure of the workpiece in the LF direction after UACFG using the SiC wheel at v_s and v_w of 15 m/s and 150 mm/min respectively. Deformation/bending of the lamellae up to ~10 μm beneath the ground surface is visible. Lamellae bending, as anticipated was less pronounced in TF sections (not subject to feed effect) such as that shown in Fig. 9(b), involving a higher cutting speed 30 m/s, however typical grit marks were visible. Similar trends were observed in workpieces ground using the EP diamond wheel, see Fig. 9(c), but with somewhat higher depth of deformation of up to ~20 μm after Test 4, due to the increased number of active grains as a result of cumulative wheel wear.
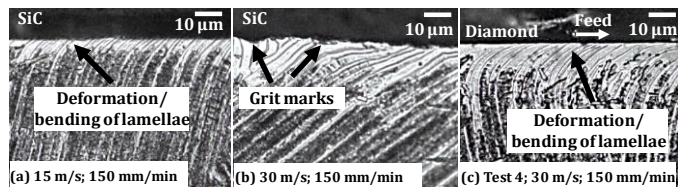
Fig. 9. Microstructures of γ-TiAl samples after UACFG with SiC wheel in (a) LF, (b) TF planes; and with diamond wheel in (c) LF plane.

4. Conclusions

When UACFG γ-TiAl, lower grinding forces were generally obtained with both vitrified SiC and EP diamond wheels compared to conventional CFG operation. With the former wheel, the normal and tangential components reduced by up to 19% and 35% respectively, while for the diamond wheel, values were 13% and 25% lower, however with uprated process parameters, the benefits of US assisted operation were less apparent. Similarly,

higher wheel G-ratios (30-75% for the SiC and 100-625% for the diamond wheel) and marginally better workpiece surface roughness/quality (~3-10% reduction in R_a) were generally observed under hybrid operating conditions. The γ-TiAl surfaces machined with UACFG displayed greater smearing, side flow/ploughing and overlapping grit marks possibly due to a change in material removal mechanism favouring a more ductile mode. Microhardness variations between conventional CFG and UACFG were minimal as were alterations of workpiece microstructure. The benefits of UACFG were not as significant as detailed in the literature involving US assisted surface grinding and it is likely that use of much higher depths of cut in UACFG hindered the translation of vibration amplitude to the cutting zone. In relation to the experimental configuration employed, ultrasonic vibration through the spindle/wheel would have been preferable in order to minimise the effects of interface damping in the workpiece-table sonotrode setup and also provide greater flexibility/scope with respect to component size/shape/mass.

References

[1] Hood R, Cooper P, Aspinwall DK, Soo SL, Lee DS (2015) Creep feed grinding of γ-TiAl using single layer electroplated diamond superabrasive wheels. *CIRP Journal of Manufacturing Science and Technology* 11:36-44.

[2] Aspinwall DK, Dewes RC, Mantle AL (2005) The Machining of γ-TiAl Intermetallic Alloys. *Annals of the CIRP* 54/1:99-104.

[3] Bentley SA, Aspinwall DK (1997) The Identification of Significant Operating Parameters When Conventional Abrasive Creep Feed Grinding a Gamma Titanium Aluminide Intermetallic. *Proceedings of the 4th International Charles Parsons Turbine Conference, Advances in Turbine Materials, Design and Manufacturing,* Newcastle Upon Tyne, UK, 474-488.

[4] Hood R, Lechner F, Aspinwall DK, Voice W (2007) Creep Feed Grinding of Gamma Titanium Aluminide and Burn Resistant Titanium Alloys Using SiC Abrasive. *International Journal of Machine Tools and Manufacture* 47:1486-1492.

[5] Lauwers B, Klocke F, Klink A, Tekkaya AE, Neugebauer R, McIntosh D (2014) Hybrid Processes in Manufacturing. *CIRP Annals – Manufacturing Technology* 63/2:561-583.

[6] Klocke F, Soo SL, Karpuschewski B, Webster JA, Novovic D, Elfizy A, Axinte DA, Tönissen S (2015) Abrasive Machining of Advanced Aerospace Alloys and Composites. *CIRP Annals – Manufacturing Technology* 64/2: 581-604.

[7] Ding K, Fu Y, Su H, Xu H, Cui F, Li Q (2017) Experimental studies on matching performance of grinding and vibration parameters in ultrasonic assisted grinding of SiC ceramics. *International Journal of Advanced Manufacturing Technology*, 88(9):2527-2535.

[8] Tawakoli T, Azarhoushang B, Rabiey M (2009) Ultrasonic Assisted Grinding of Soft Steel. *Industrial Diamond Quarterly* 1:40-44.

[9] Bhaduri D, Soo SL, Aspinwall DK, Novovic D, Harden P, Bohr S, Martin D (2012) A Study on Ultrasonic Assisted Creep Feed Grinding of Nickel Based Superalloys. *Procedia CIRP* 1:359-364.

[10] Bhaduri D, Soo SL, Novovic D, Aspinwall DK, Harden P, Waterhouse C, Bohr S, Mathieson AC, Lucas M (2013) Ultrasonic Assisted Creep Feed Grinding of Inconel 718. *Procedia CIRP* 6:615-620.

[11] Webster JA (2007) Improving Surface Integrity and Economics of Grinding by Optimum Coolant Application, with Consideration of Abrasive Tool and Process Regime. *Proceedings of the Institution of Mechanical Engineers, Part B: Journal of Engineering Manufacture* 221(12):1665-1675.

[12] Hood R, Aspinwall DK, Voice W (2007) Creep Feed Grinding of a Gamma Titanium Aluminide Intermetallic Alloy Using SiC Abrasives. *Journal of Materials Processing Technology* 191:210-214.

[13] Nik MG, Movahhedy MR, Akbari J (2012) Ultrasonic-Assisted Grinding of Ti6Al4V Alloy. *Procedia CIRP* 1:370-375.

[14] Zhang, H, Zhang J (2009) Separate critical condition for ultrasonic vibration assisted grinding. *Journal of Shanghai University* 13(5):391-395.

[15] Gao GF, Zhao B, Xiang DH, Kong QH (2009) Research on the Surface Characteristics in Ultrasonic Grinding Nano-Zirconia Ceramics. *Journal of Materials Processing Technology* 209:32-37.

[16] Sharman ARC, Li XP, Rahman M, Bowen P, Dewes RC, Aspinwall DK (2001) Ultrasonic Assisted Turning of Gamma Titanium Aluminide. *Proceedings of the Thirteenth International Symposium for Electromachining – ISEM XIII (Vol. 2)*, Bilbao, Spain, 939-951.